Cutting Data and Grinding

Dr Mirza Jahanzaib

Cutting Data

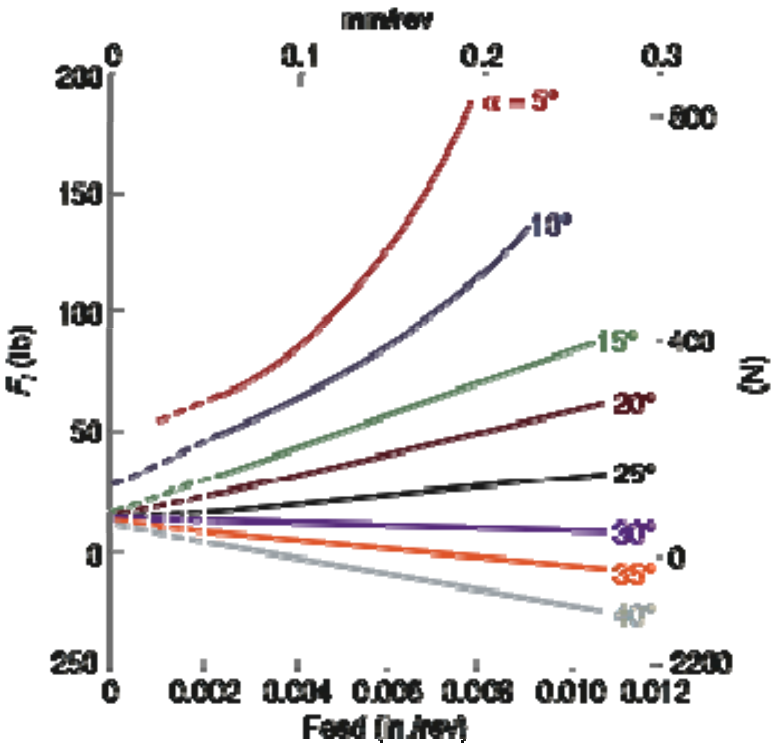

TABLE 8.1 Data on orthogonal cutting of 4130 steel.

α	φ	γ	μ	β	F_c (lb)	F_t (lb)	u_c (in.-lb/in.^{3} × 10^3)	u_s	u_f	u_f/u_c (%)
25°	30.9°	2.33	1.46	56	380	224	320	209	111	35
35	31.6	1.86	1.53	57	264	102	214	112	102	48
40	33.7	1.32	1.54	57	272	71	196	94	101	52
45	41.9	1.06	1.53	62	272	68	196	73	120	62

t_o = 0.0023 in.; w = 0.475 in.; V = 90 ft/min; tool: high-speed steel.

TABLE 8.2 Data on orthogonal cutting of 9445 steel.

α	V	φ	γ	μ	β	F_c	F_t	u_c	u_s	u_f	u_f/u_c (%)
+10	197	17	3.4	1.05	48	370	273	400	292	108	27
	400	19	3.1	1.11	48	360	283	390	266	124	32
	642	21.5	2.7	0.95	44	320	217	356	249	107	30
	1186	25	2.4	0.91	30	303	168	328	225	103	31
-10	400	16.5	3.9	0.64	33	416	385	450	342	108	24
	637	19	3.5	0.59	30	384	326	415	312	103	25
	1160	22	3.1	0.51	27	356	263	385	289	96	25

t_o = 0.037 in.; w = 0.25 in.; tool: cemented carbide.

Thrust force as a function of rake angle and feed in orthogonal cutting of AISI 1112 cold-rolled steel. Note that at high rake angles, the thrust force is negative. A negative thrust force has important implications in the design of machine tools and in controlling the stability of the cutting process.
Source: **After S. Kobayashi and E.G. Thomsen.**

Shear Force & Normal Force

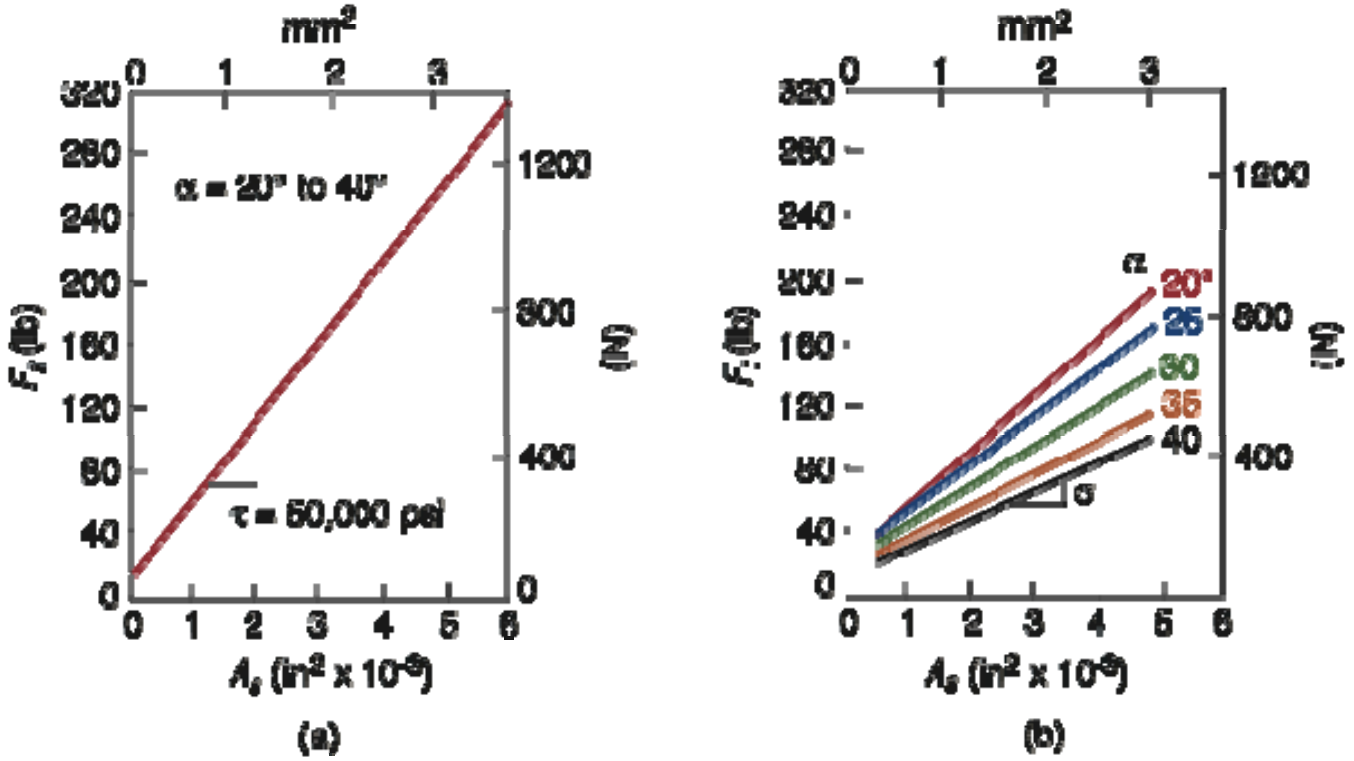

(a) Shear force

(b) normal force as a function of the area of the shear plane and the rake angle for 85-15 brass. Note that the shear stress in the shear plane is constant, regardless of the magnitude of the normal stress, indicating that the normal stress has no effect on the shear flow stress of the material.

Source: After S. Kobayashi and E.G. Thomsen.

Shear Stress on Tool Face

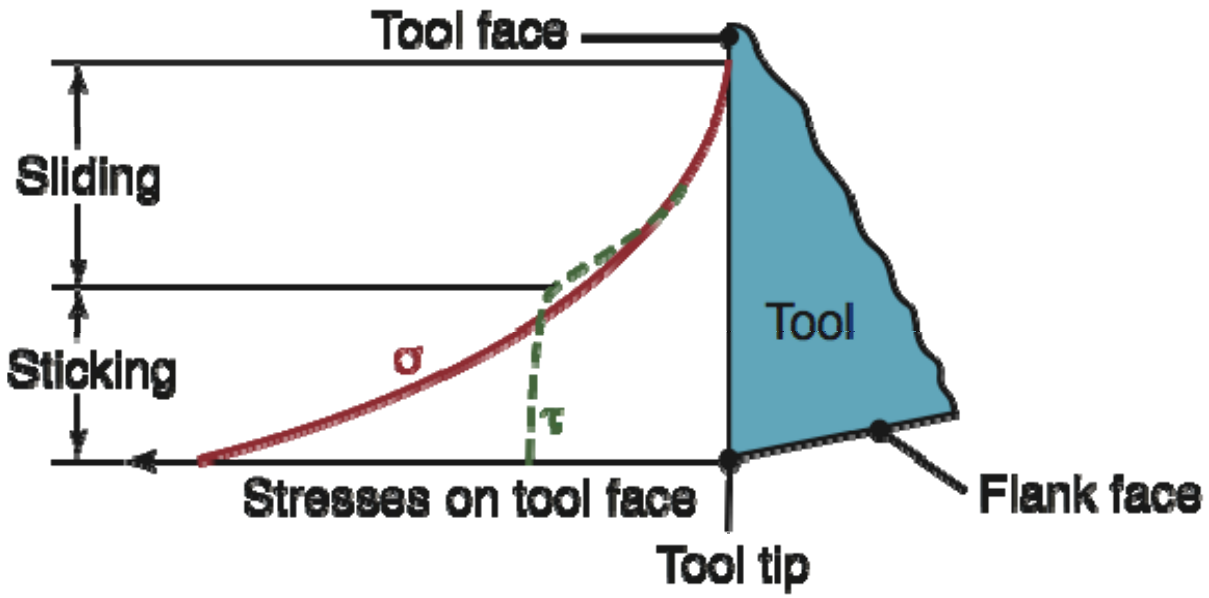

Schematic illustration of the distribution of normal and shear stresses at the tool-chip interface (rake face).

Note that, whereas the normal stress increases continuously toward the tip of the tool, the shear stress reaches a maximum and remains at that value (a phenomenon known as *sticking*; see Section 4.4.1).

Shear-Angle Relationships

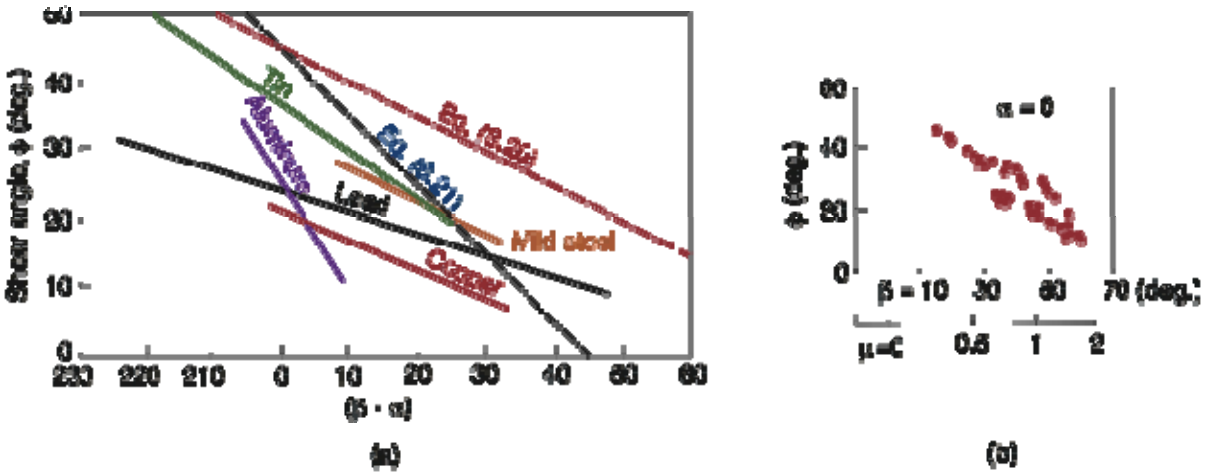

(a) Comparison of experimental and theoretical shear-angle relationships. More recent analytical studies have resulted in better agreement with experimental data.
(b) Relation between the shear angle and the friction angle for various alloys and cutting speeds. ***Source:*** **After S. Kobayashi.**

Merchant [Eq. (8.20)]

$$\phi = 45^\circ + \frac{\alpha}{2} - \frac{\beta}{2}$$

Shaffer [Eq. (8.21)]

$$\phi = 45^\circ + \alpha - \beta$$

Mizuno [Eqs. (8.22)-(8.23]

$$\phi = \alpha \quad \text{for} \quad \alpha > 15^\circ$$

$$\phi = 15^\circ \quad \text{for} \quad \alpha < 15^\circ$$

Specific Energy

Material	Specific Energy* W-s/mm^3	hp-min/in^3
Aluminum alloys	0.4-1.1	0.15-0.4
Cast irons	1.6-5.5	0.6-2.0
Copper alloys	1.4-3.3	0.5-1.2
High-temperature alloys	3.3-8.5	1.2-3.1
Magnesium alloys	0.4-0.6	0.15-0.2
Nickel alloys	4.9-6.8	1.8-2.5
Refractory alloys	3.8-9.6	1.1-3.5
Stainless steels	3.0-5.2	1.1-1.9
Steels	2.7-9.3	1.0-3.4
Titanium alloys	3.0-4.1	1.1-1.5

* At drive motor, corrected for 80% efficiency; multiply the energy by 1.25 for dull tools.

TABLE 8.3 Approximate Specific-Energy Requirements in Machining Operations

Example 8.1: Frictional energy in cutting

We are carrying out an orthogonal cutting process in which t_o =0.005 in., V= 400 ft/min, $\alpha=10^o$, and the width of cut =0.25in. We observe that t_c= 0.009 in. ,F_c=125 lb, and F_t = 50 lb.

We want to calculate the percentage of the total energy that goes into overcoming friction at the tool-chip interface.

Where

SOLUTION.

We can express the percentage as:

$$\frac{Friction\ energy}{Total\ energy} = \frac{FV_c}{F_cV} = \frac{F_r}{F_c}$$

Where

$$r = \frac{t_o}{t_c} = \frac{5}{9} = 0.555, \qquad F = R\sin\beta, \qquad F_c = R\cos(\beta - \alpha)$$

$$R = \sqrt{F_t^2 + F_c^2} = \sqrt{50^2 + 125^2} = 135Ib$$

Thus

$$125 = 135\cos(\beta - 10)$$

from which

$$\beta = 32^o \text{ and } F = 135\sin 32^o = 71.5lb$$

Hence

$$Percenentage = \frac{(71.5)(0.555)}{125} = 0.32 = 32\%$$

Grinding and Abrasives

- When the material is either too hard or brittle, or the shape is difficult to produce, with dimensional accuracy by the one of the machining processes as described in previous chapter, ***abrasives are used***.
- Abrasive machining processes are generally among the ***last operations performed*** on manufactured products.

Types of Abrasives

- Conventional abrasives:
  - **Aluminium oxide**
  - **Silicon carbide**
- Super abrasives
  - **Cubic boron nitride**
  - **Diamond**

In addition to hardness, an important characteristic of an abrasive is ***friability.***

Friability is the ability of an abrasive grain to fracture into smaller pieces. Friability gives abrasives self sharpening characteristics which are important in maintaining the sharpness of abrasives during use. The **shape and size** of abrasive grain also affect its friability.

Typical Grinding wheel

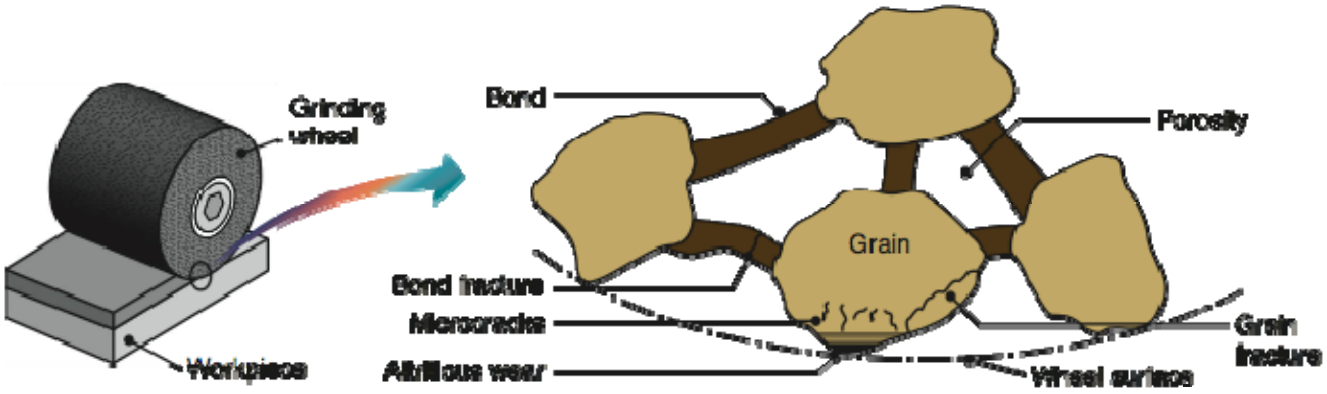

FIGURE 9.1 Schematic illustration of a physical model of a grinding wheel, showing its structure and grain wear and fracture patterns.

TABLE 9.1 Knoop hardness range for various materials and abrasives.

Common glass	350-500	Titanium nitride	2000
Flint, quartz	800-1100	Titanium carbide	1800-3200
Zirconium oxide	1000	Silicon carbide	2100-3000
Hardened steels	700-1300	Boron carbide	2800
Tungsten carbide	1800-2400	Cubic boron nitride	4000-5000
Aluminum oxide	2000-3000	Diamond	7000-8000

Grinding Wheel Types, super abrasives and Marking systems

- Grinding Wheel Types

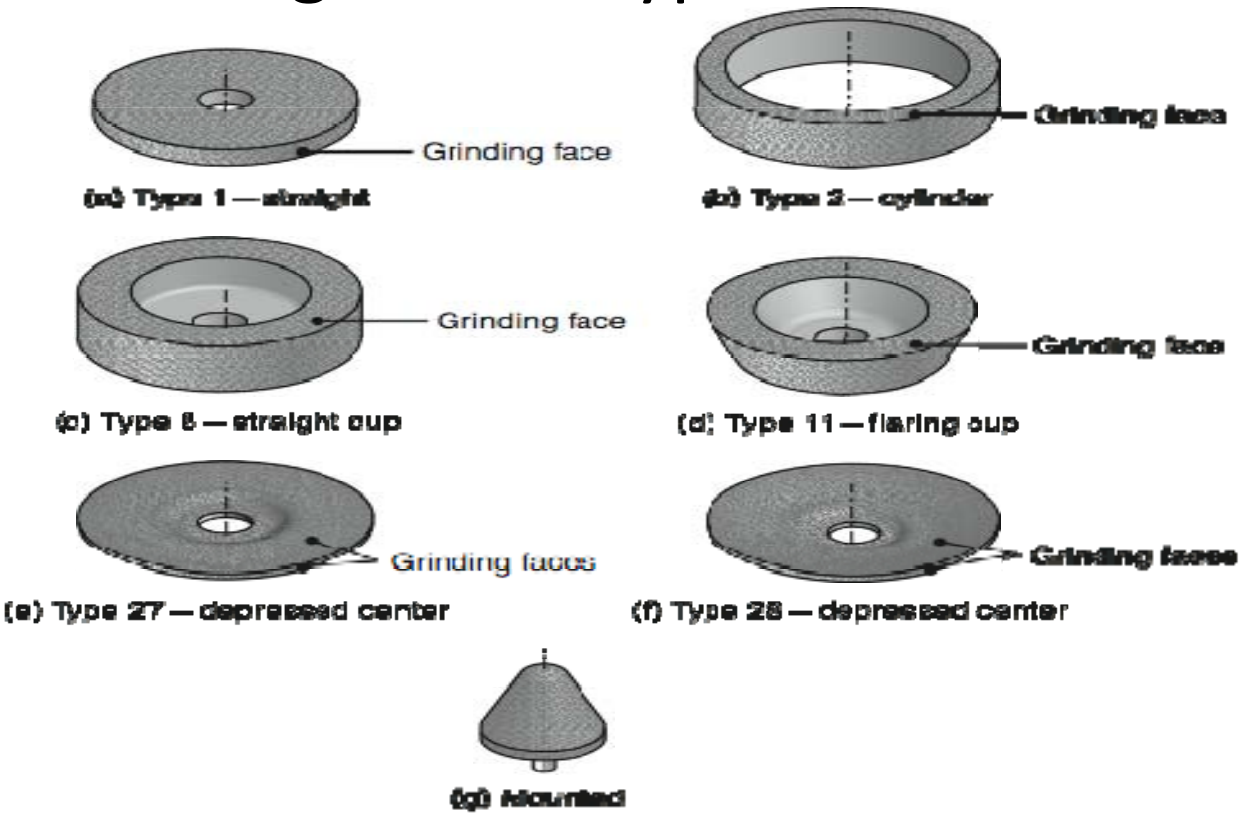

FIGURE 9.2 Some common types of grinding wheels made with conventional abrasives (aluminum oxide and silicon carbide). Note that each wheel has a specific grinding face; grinding on other surfaces is improper and unsafe.

Super abrasives

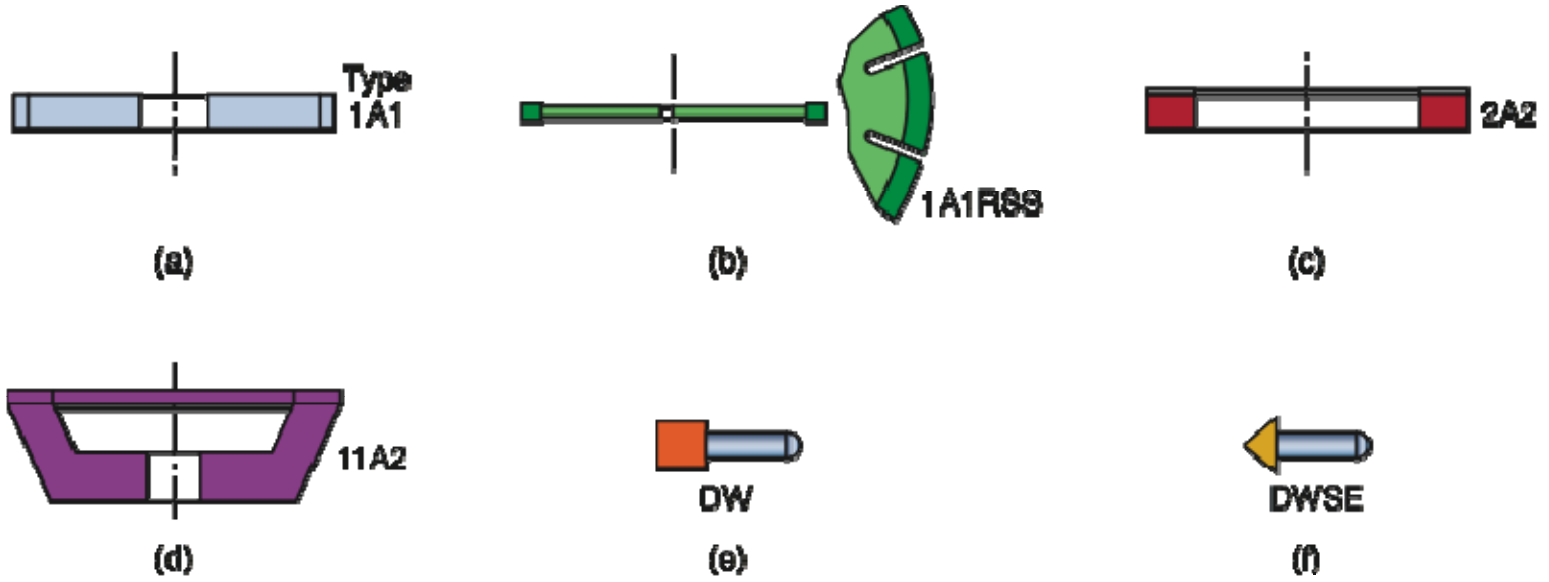

FIGURE 9.3 Examples of superabrasive wheel configurations. The rim consists of superabrasives and the wheel itself (core) is generally made of metal or composites. Note that the basic numbering of wheel types (such as 1, 2, and 11) is the same as that shown in Fig. 9.2. The bonding materials for the superabrasives are: (a), (d), and (e) resinoid, metal, or vitrified; (b) metal; (c) vitrified; and (f) resinoid.

Grinding wheel Marking system

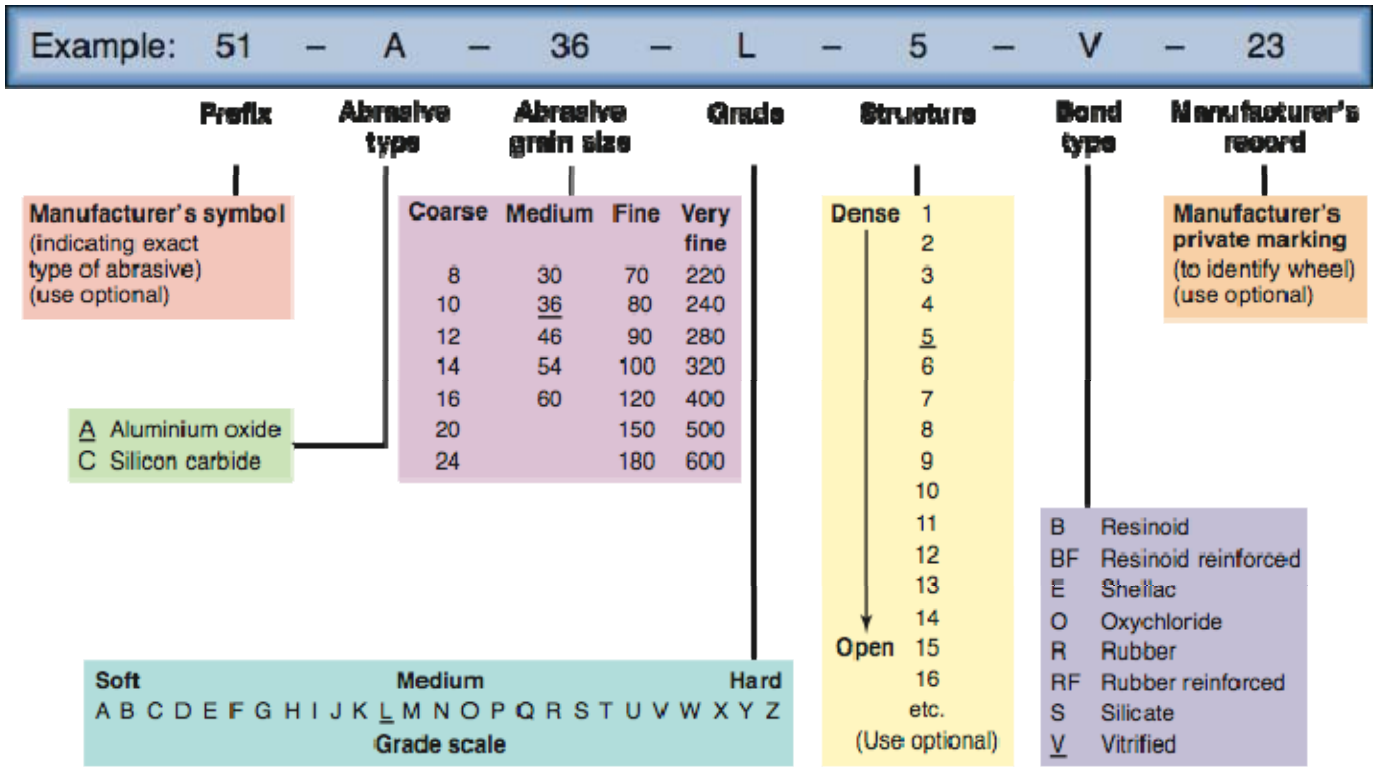

FIGURE 9.4 Standard marking system for aluminum-oxide and silicon-carbide bonded abrasives.

Diamond and cBN marking system

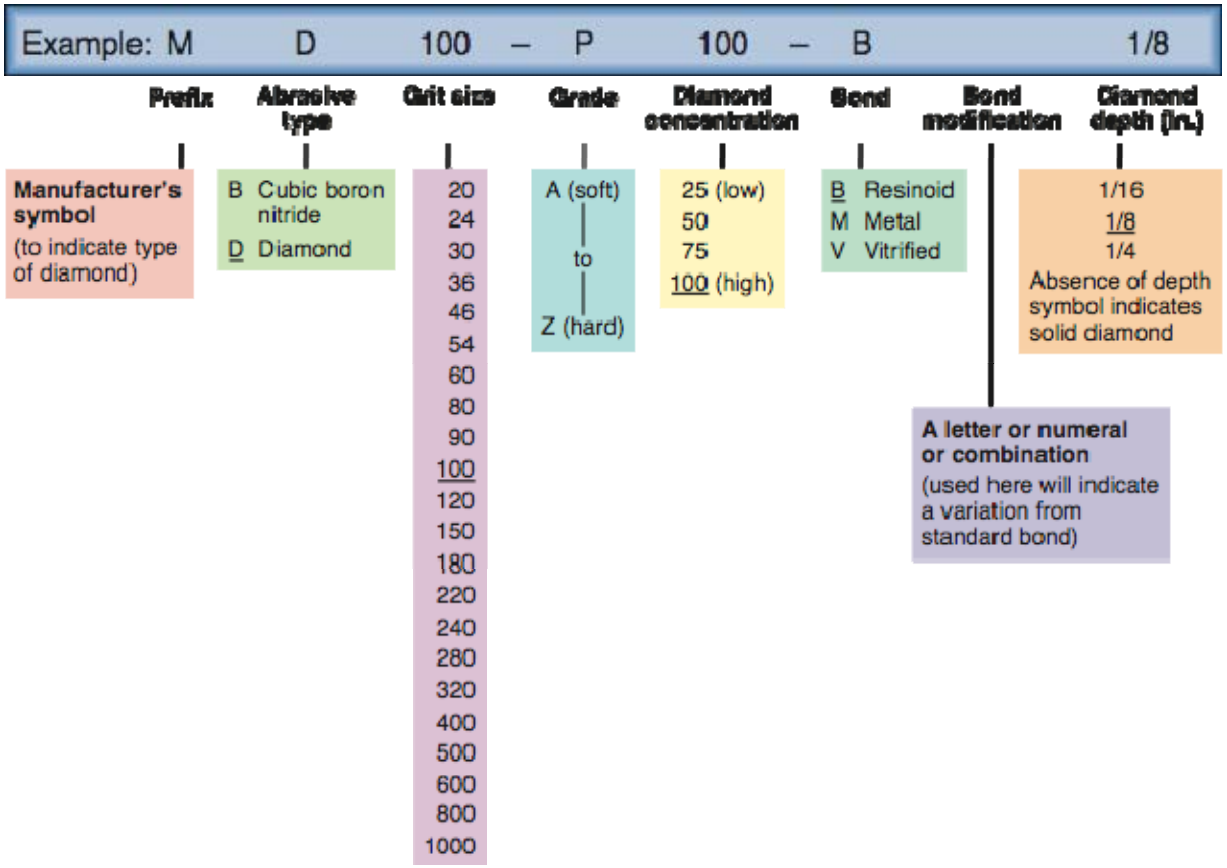

FIGURE 9.5 Standard marking system for diamond and cubic-boron-nitride bonded abrasives.

Mechanics of Grinding

- Grinding is basically a chip removal process in which the cutting tool is an individual abrasive grain. It differs from single point cutting tool as:

  - The individual grain has irregular geometry

  - The average rake angle of the grains is highly negative i.e. -60 degree or even lower

  - The grains on the periphery of a grinding wheel has different radial positions

  - The cutting speed of the grinding wheels are very high i.e. 30m/s (6000 ft/min)

An example of chip formation by an abrasive grain is shown in figure below: From the figure it is noted that a variety of metals chips are obtained.

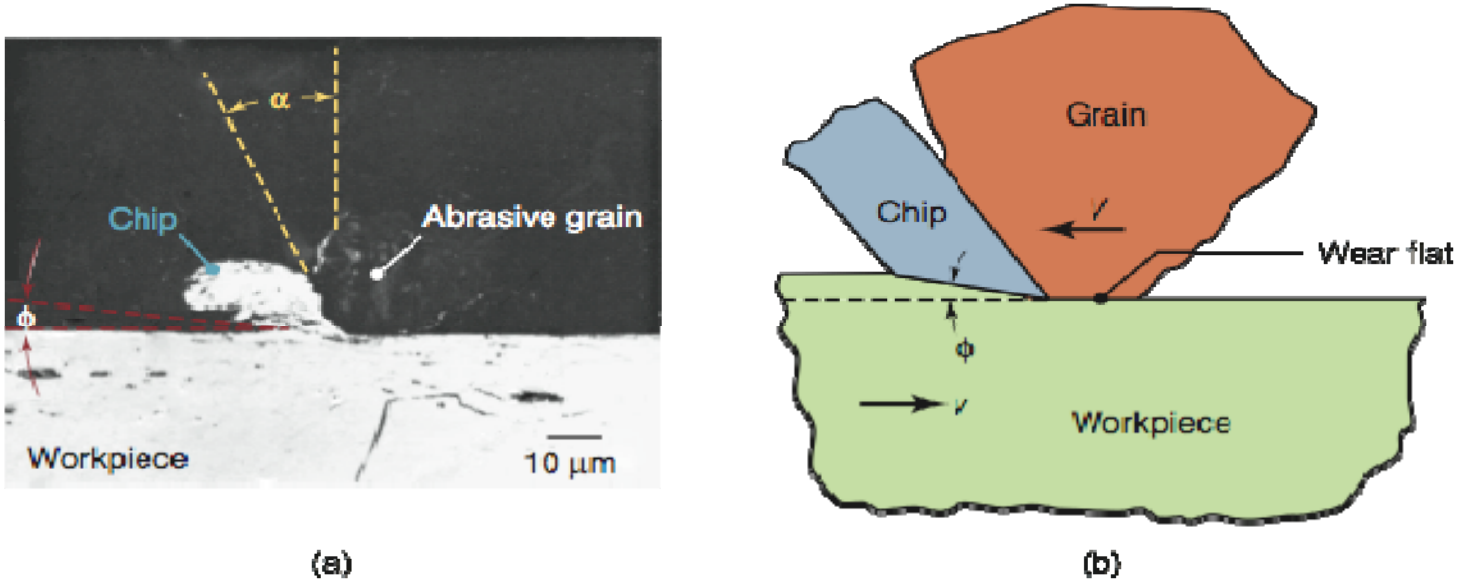

FIGURE 9.7 (a) Grinding chip being produced by a single abrasive grain. Note the large negative rake angle of the grain. *Source*: After M.E. Merchant. (b) Schematic illustration of chip formation by an abrasive grain. Note the negative rake angle, the small shear angle, and the wear flat on the grain.

The mechanics of grinding and variables can best be studied by analyzing the surface grinding operations as shown below:

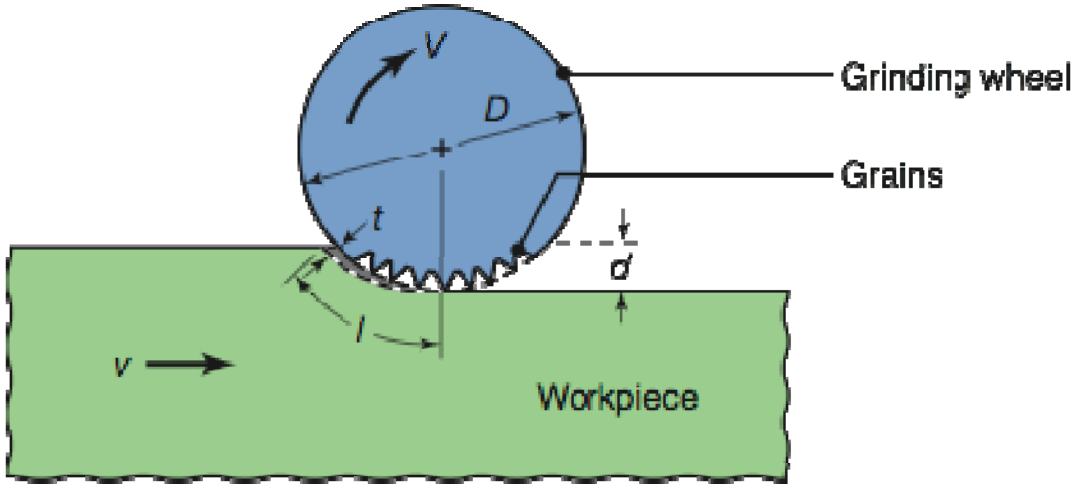

FIGURE 9.8 Basic variables in surface grinding. In actual grinding operations, the wheel depth of cut, *d*, and contact length, *l*, are much smaller than the wheel diameter, *D*. The dimension *t* is called the *grain depth of cut*.

In figure, a grinding wheel of diameter D is removing a layer of metal of depth d, ***known as wheel depth of cut***.

An individual grain on the periphery of the **wheel is moving at a tangential velocity V** and **work piece is moving with velocity v**.

The grain is removing a chip of an un-deformed thickness (grain depth of cut), t, and un-deformed length l.

For the condition of v<<V, the un-deformed chip length is approximately

$$l \simeq \sqrt{Dd}$$

For external (cylindrical) grinding

$$l = \sqrt{\frac{Dd}{1+(D/D_w)}}$$

For internal grinding

$$t = \sqrt{\frac{Dd}{1-(D/D_w)}}$$

Where D**w** is the diameter of the work piece.

The relationship between **t** and other process variables can be derived as follows:

Let **C** = Number of cutting points per unit area of wheel surface

V and v = Surface speeds of the wheel and work piece

w = width of work piece to be unity

Number of grinding chips produced per unit time is **VC**

Volume of material removed per unit time = **vd**

letting also that **r** be the ratio of chip width, **w**, to the average chip thickness, then volume of chip with rectangular cross sectional area and constant width along its length is

$$\text{Vol}_{\text{chip}} = \frac{wtl}{2} = \frac{rt^2 l}{4}$$

The volume of material removed per unit time is the product of the volume of each chip and the number of chip produced per unit time.

Thus

$$VC\,\frac{rt^2 l}{4} = vd$$

And because l = $\sqrt{Dd}$

the un-deformed chip thickness in the surface grinding is

$$t = \sqrt{\frac{4v}{VCr}\sqrt{\frac{d}{D}}}$$

Example 9.1

Estimate the un-deformed chip length and the un-deformed chip thickness for a typical surface grinding operation. Let

D = 200 mm, d = 0.05 mm, C = 2 per mm^2, and r = 15

Solution

The formula for un-deformed length and thickness respectively are

$l = \sqrt{Dd}$ and $t = \sqrt{4v/VCr\sqrt{d/D}}$

From table 9.2, the following values are selected:

v = 0.5 m/s and V = 30m/s

Therefore, $l = \sqrt{(200)(0.05)}$ = 3.2 mm = 0.126 in

And

$t = \sqrt{(4)(0.5)/(30)(2)(15)\sqrt{0.05/200}}$ = 0.006 mm = 2.3×10^{-4} in

Note that due to plastic deformation, the actual length of the chip is shorter and the thickness greater than these values

Grinding forces

The knowledge of force is essential for the deflections that the work piece and machine will undergo. If we assume that force on the grain is proportional to the cross-sectional area of the un-deformed chip, it can be shown that the relative grain force is given by

Relative grain force $\propto \frac{v}{VC}\sqrt{d/D}$

The specific energy consumed in producing a grinding chip consists of three components.

$$u = u_{chip} + u_{plowing} + u_{sliding}$$

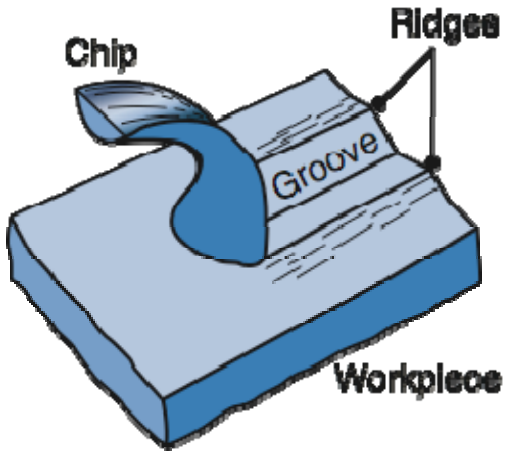

FIGURE 9.9 Chip formation and plowing (plastic deformation without chip removal) of the workpiece surface by an abrasive grain.

TABLE 9.2 Typical ranges of speeds and feeds for abrasive processes.

Process Variable	Conventional Grinding	Creep-Feed Grinding	Buffing	Polishing
Wheel speed (m/min)	1500 3000	1500 3000	1800 3600	1500-2400
Work speed (m/min)	10-60	0.1-1	-	-
Feed (mm/pass)	0.01-0.05	1-6	-	-

		Specific Energy	
Workpiece Material	Hardness	W-s/mm^3	hp-min/in^3
Aluminum	150 HB	7-27	2.5-10
Cast iron (class 40)	215 HB	12 60	4.5 22
Low-carbon steel (1020)	110 HB	14-68	5-25
Titanium alloy	300 HB	16-55	6-20
Tool steel (T15)	67 HRC	18-82	6.5-30